

# The ASAS-SN Bright Supernova Catalog – IV. 2017

T. W.-S. Holoiën<sup>1\*</sup>, J. S. Brown<sup>2,3</sup>, P. J. Vallely<sup>2</sup>, K. Z. Stanek<sup>2,4</sup>,  
 C. S. Kochanek<sup>2,4</sup>, B. J. Shappee<sup>5</sup>, J. L. Prieto<sup>6,7</sup>, Subo Dong<sup>8</sup>, J. Brimacombe<sup>9</sup>,  
 D. W. Bishop<sup>10</sup>, S. Bose<sup>8</sup>, J. F. Beacom<sup>2,4,11</sup>, D. Bersier<sup>12</sup>, Ping Chen<sup>8</sup>,  
 L. Chomiuk<sup>13</sup>, E. Falco<sup>14</sup>, T. Jayasinghe<sup>2</sup>, N. Morrell<sup>15</sup>, G. Pojmanski<sup>16</sup>,  
 J. V. Shields<sup>2</sup>, J. Strader<sup>13</sup>, M. D. Stritzinger<sup>17</sup>, Todd A. Thompson<sup>2,4</sup>,  
 P. R. Woźniak<sup>18</sup>, P. Cacella<sup>19</sup>, J. G. Carballo<sup>20</sup>, E. Conseil<sup>21</sup>, I. Cruz<sup>22</sup>,  
 R. G. Farfan<sup>23</sup>, J. M. Fernandez<sup>24</sup>, S. Kiyota<sup>25</sup>, R. A. Koff<sup>26</sup>, G. Krannich<sup>27</sup>,  
 P. Marples<sup>28</sup>, G. Masi<sup>29</sup>, L. A. G. Monard<sup>30</sup>, B. Nicholls<sup>31</sup>, R. S. Post<sup>32</sup>,  
 G. Stone<sup>33</sup>, D. L. Trappett<sup>34</sup>, and W. S. Wiethoff<sup>35</sup>

<sup>1</sup> *The Observatories of the Carnegie Institution for Science, 813 Santa Barbara Street, Pasadena, CA 91101, USA*

<sup>2</sup> *Department of Astronomy, The Ohio State University, 140 West 18th Avenue, Columbus, OH 43210, USA*

<sup>3</sup> *Department of Astronomy and Astrophysics, University of California, Santa Cruz, CA 92064, USA*

<sup>4</sup> *Center for Cosmology and AstroParticle Physics (CCAPP), The Ohio State University, 191 W. Woodruff Ave., Columbus, OH 43210, USA*

<sup>5</sup> *Institute for Astronomy, University of Hawai'i, 2680 Woodlawn Drive, Honolulu, HI 96822, USA*

<sup>6</sup> *Núcleo de Astronomía de la Facultad de Ingeniería y Ciencias, Universidad Diego Portales, Av. Ejército 441, Santiago, Chile*

<sup>7</sup> *Millennium Institute of Astrophysics, Santiago, Chile*

<sup>8</sup> *Kaoli Institute for Astronomy and Astrophysics, Peking University, Yi He Yuan Road 5, Hai Dian District, Beijing 100871, China*

<sup>9</sup> *Coral Towers Observatory, Cairns, Queensland 4870, Australia*

<sup>10</sup> *Rochester Academy of Science, 1194 West Avenue, Hilton, NY 14468, USA*

<sup>11</sup> *Department of Physics, The Ohio State University, 191 W. Woodruff Ave., Columbus, OH 43210, USA*

<sup>12</sup> *Astrophysics Research Institute, Liverpool John Moores University, 146 Brownlow Hill, Liverpool L3 5RF, UK*

<sup>13</sup> *Department of Physics and Astronomy, Michigan State University, East Lansing, MI 48824, USA*

<sup>14</sup> *Harvard-Smithsonian Center for Astrophysics, 60 Garden St., Cambridge, MA 02138, USA*

<sup>15</sup> *Las Campanas Observatory, Carnegie Observatories, Casilla 601, La Serena, Chile*

<sup>16</sup> *Warsaw University Astronomical Observatory, Al. Ujazdowskie 4, 00-478 Warsaw, Poland*

<sup>17</sup> *Department of Physics and Astronomy, Aarhus University, Ny Munkegade 120, DK-8000 Aarhus C, Denmark*

<sup>18</sup> *Los Alamos National Laboratory, Mail Stop B244, Los Alamos, NM 87545, USA*

<sup>19</sup> *DogsHeaven Observatory, SMPW Q25 C/J1 LT10B, Brasilia, DF 71745-501, Brazil*

<sup>20</sup> *Observatorio Cerro del Viento-MPC 184, Paseo Condes de Barcelona, 6-4D, 06010 Badajoz, Spain*

<sup>21</sup> *Association Francaise des Observateurs d'Etoiles Variables (AFOEV), Observatoire de Strasbourg, 11 Rue de l'Université, 67000 Strasbourg, France*

<sup>22</sup> *Cruz Observatory, 1971 Haverton Drive, Reynoldsburg, OH 43068, USA*

<sup>23</sup> *Uraniborg Observatory, cija, Sevilla, Spain*

<sup>24</sup> *Observatory Inmaculada del Molino, Hernando de Esturmio 46, Osuna, 41640 Sevilla, Spain*

<sup>25</sup> *Variable Star Observers League in Japan, 7-1 Kitahatsutomi, Kamagaya, Chiba 273-0126, Japan*

<sup>26</sup> *Antelope Hills Observatory, 980 Antelope Drive West, Bennett, CO 80102, USA*

<sup>27</sup> *Roof Observatory Kaufering, Lessingstr. 16, D-86916 Kaufering, Germany*

<sup>28</sup> *Leyburn & Loganholme Observatories, 45 Kiewa Drive, Loganholme, Queensland 4129, Australia*

<sup>29</sup> *Virtual Telescope Project, Via Madonna de Loco, 47-03023 Ceccano (FR), Italy*

<sup>30</sup> *Kleinkaroo Observatory, Calitzdorp, St. Helena 1B, P.O. Box 281, 6660 Calitzdorp, Western Cape, South Africa*

<sup>31</sup> *Mount Vernon Observatory, 6 Mount Vernon Place, Nelson, New Zealand*

<sup>32</sup> *Post Observatory, Lexington, MA 02421, USA*

<sup>33</sup> *Sierra Remote Observatories, 44325 Alder Heights Road, Auberry, CA 93602, USA*

<sup>34</sup> *Brisbane Girls Grammar School - Dorothy Hill Observatory, Gregory Terrace, Spring Hill, Queensland 4000, Australia*

<sup>35</sup> *Department of Earth and Environmental Sciences, University of Minnesota, 230 Heller Hall, 1114 Kirby Drive, Duluth, MN. 55812, USA*

18 May 2022

**ABSTRACT**

In this catalog we compile information for all supernovae discovered by the All-Sky Automated Survey for SuperNovae (ASAS-SN) as well as all other bright ( $m_{peak} \leq 17$ ), spectroscopically confirmed supernovae found in 2017, totaling 308 supernovae. We also present UV through near-IR magnitudes gathered from public databases of all host galaxies for the supernovae in the sample. We perform statistical analyses of our full bright supernova sample, which now contains 949 supernovae discovered since 2014 May 1, including supernovae from our previous catalogs. This is the fourth of a series of yearly papers on bright supernovae and their hosts from the ASAS-SN team.

**Key words:** supernovae, general — catalogues — surveys

**1 INTRODUCTION**

In recent years, large-scale, systematic surveys for supernovae (SNe) and other transient phenomena have become a cornerstone of modern astronomy. Significant examples of such surveys include the Lick Observatory Supernova Search (LOSS; Li et al. 2000), the Panoramic Survey Telescope & Rapid Response System (Pan-STARRS; Kaiser et al. 2002), the Texas Supernova Search (Quimby 2006), the Sloan Digital Sky Survey (SDSS) Supernova Survey (Frieman et al. 2008), the Catalina Real-Time Transient Survey (CRTS; Drake et al. 2009), the CHilean Automatic Supernova sEarch (CHASE; Pignata et al. 2009), the Palomar Transient Factory (PTF; Law et al. 2009), the Gaia transient survey (Hodgkin et al. 2013), the La Silla-QUEST (LSQ) Low Redshift Supernova Survey (Baltay et al. 2013), the Mobile Astronomical System of TELEscope Robots (MASTER; Gorbovskoy et al. 2013) survey, the Optical Gravitational Lensing Experiment-IV (OGLE-IV; Wyrzykowski et al. 2014), the Asteroid Terrestrial-impact Last Alert System (ATLAS; Tonry 2011; Tonry et al. 2018), and the Zwicky Transient Facility (ZTF).

Despite the large number of transient surveys, however, prior to 2013 there was no high-cadence optical survey designed to survey the entire visible sky to find the bright, nearby transients that can be observed in the greatest detail. Such events, while fewer in number, provide the opportunity to obtain the high-quality observational data needed to have the largest impact on our understanding of the physics behind transient phenomena.

The All-Sky Automated Survey for SuperNovae (ASAS-SN<sup>1</sup>; Shappee et al. 2014) was created for this purpose. ASAS-SN is designed to survey the entire visible sky at a rapid cadence to find the brightest transients. ASAS-SN has found many nearby and interesting SNe (e.g., Dong et al. 2016; Holoien et al. 2016a; Shappee et al. 2016; Godoy-Rivera et al. 2017; Bose et al. 2018b,a; Vallely et al. 2018), tidal disruption events (TDEs; e.g., Holoien et al. 2014a; Brown et al. 2016; Holoien et al. 2016c,b; Prieto et al. 2016; Romero-Cañizales et al. 2016; Brown et al. 2017a; Holoien et al. 2018), stellar outbursts (Holoien et al. 2014b; Schmidt et al. 2014; Herczeg et al. 2016; Schmidt et al. 2016), flares from active galactic nuclei (Shappee et al. 2014), black hole

binaries (Tucker et al. 2018), and cataclysmic variable stars (Kato et al. 2014a,b, 2015, 2016).

Each ASAS-SN unit is hosted by the Las Cumbres Observatory (Brown et al. 2013) network and consists of four 14-cm telescopes, each with a  $4.5 \times 4.5$  degree field-of-view. Until 2017, ASAS-SN comprised two units, each using  $V$ -band filters with a limiting magnitude of  $m_V \sim 17$ : Brutus, located on Haleakala in Hawaii, and Cassius, located at Cerro Tololo, Chile (see Shappee et al. (2014) for further technical details). In late 2017, ASAS-SN expanded with three new units: Paczynski, also located at Cerro Tololo, Leavitt, located at McDonald Observatory in Texas, and Payne-Gaposchkin, located in Sutherland, South Africa. Between the five units, ASAS-SN can now cover the entire observable sky (roughly 30000 square degrees) in less than a single night, with weather losses. Further, ASAS-SN switched to  $g$ -band for our new units, increasing our limiting magnitude to  $m_g \sim 18.5$ . Due to the increased depth, we will be switching our initial 8 telescopes to  $g$ -band as well by the end of 2018. For a more detailed history of the ASAS-SN project, see Holoien et al. (2017a) and Shappee et al. (2014).

All ASAS-SN data are automatically processed and are searched in real-time, with all discoveries being announced publicly if obvious or upon confirmation. This allows for both rapid discovery and response by the ASAS-SN team, as well as by others. The untargeted approach used by ASAS-SN and its 97% spectroscopic confirmation makes the ASAS-SN sample much less biased than many other SN searches. The ASAS-SN sample is thus ideal for population studies of nearby SNe and their hosts (e.g., Brown et al. 2018).

This manuscript is the fourth of a series of yearly catalogs provided by the ASAS-SN team. We present collected information on all SNe discovered by ASAS-SN in 2017 and their host galaxies. We also provide the same information for all bright SNe (those with  $m_{peak} \leq 17$ ) discovered by other professional and amateur astronomers in the same year, as we have done with our previous catalogs (Holoien et al. 2017a,b,c). We also include whether ASAS-SN independently recovered these SNe after their initial discovery, to better quantify the completeness of our survey.

The analyses and information presented in this paper supersede information contained in discovery and classification Astronomer’s Telegrams (ATels), which are cited in this manuscript, and the publicly available information on

\* tholoien@carnegiescience.edu

<sup>1</sup> <http://www.astronomy.ohio-state.edu/~assassin/>

ASAS-SN webpages and the Transient Name Server (TNS<sup>2</sup>). As a reminder, the proper name of any ASAS-SN transient is the ASAS-SN name. We participate in the TNS system to avoid confusion but strongly object to a naming scheme that does not credit the discoverer, even though this would be trivial to implement.

The catalog is organized as follows: in Section 2 we describe the sources of the information presented in this manuscript and list SNe with updated classifications and redshift measurements. In Section 3, we give statistics on the supernova and host galaxy populations in our full cumulative sample, including the discoveries listed in Holoien et al. (2017a,b,c), and discuss overall trends in the sample. Throughout our analyses, we assume a standard  $\Lambda$ CDM cosmology with  $H_0 = 69.3 \text{ km s}^{-1} \text{ Mpc}^{-1}$ ,  $\Omega_M = 0.29$ , and  $\Omega_\Lambda = 0.71$  for converting host redshifts into distances. In Section 4, we summarize our overall findings and discuss future directions for the ASAS-SN survey and how they will impact future discoveries.

## 2 DATA SAMPLES

Below we outline the sources of the data collected in our supernova and host galaxy samples. These data are presented in Tables 1, 2, 3, and 4.

### 2.1 The ASAS-SN Supernova Sample

All information for supernovae discovered by ASAS-SN between 2017 January 1 and 2017 December 31 is given in Table 1. As in Holoien et al. (2017a,b,c), we obtained all supernova names, discovery dates, and host names from our discovery ATels, which are cited in Table 1. Also included in the table are the IAU names given to each supernova by TNS, which is the official mechanism for reporting new astronomical transients to the IAU. ASAS-SN continues to participate in the TNS system to avoid potential confusion over discoveries, but throughout this catalog we use the internal survey discovery names for each supernova as our primary nomenclature, and we encourage others to do the same to preserve the origins of new transients in future literature.

We measured all ASAS-SN supernova redshifts from classification spectra. For cases where the nominal supernova host galaxy had a previously measured redshift that is consistent with the transient redshift, we list the redshift of the host taken from the NASA/IPAC Extragalactic Database (NED)<sup>3</sup>. For other cases, we report the redshifts given in the classification telegrams or posted on TNS, with the exception of those that are updated in this work (see below).

Classifications for ASAS-SN supernova discoveries were retrieved from classification telegrams, which are cited in Table 1 when available, or from TNS, when a classification was not reported in an ATel. We list ‘‘TNS’’ in the ‘‘Classification Telegram’’ column of the table for such cases. When measurable from the classification spectra, we also give the approximate age of the SN at discovery in days relative to peak.

Classifications were typically obtained using either the Supernova Identification code (SNID; Blondin & Tonry 2007) or the Generic Classification Tool (GELATO<sup>4</sup>; Harutyunyan et al. 2008), which both compare observed input spectra to template spectra in order to estimate the supernova age and type.

Based on re-examining archival classification spectra of ASAS-SN discoveries available on TNS and the Weizmann Interactive Supernova data REpository (WISEREP; Yaron & Gal-Yam 2012), we update a number of redshifts and classifications that differ from what was previously reported. ASASSN-17bb, ASASSN-17ol, and ASASSN-17om have updated redshifts, and ASASSN-17io has an updated type based on archival spectra. We also report the classifications (and in some cases, redshifts) for a number of supernovae that were not previously publicly classified based on spectra obtained with the Wide Field Reimaging CCD Camera (WFCCD) mounted on the Las Campanas Observatory du Pont 2.5-m telescope and the Fast Spectrograph (FAST; Fabricant et al. 1998) mounted on the Fred L. Whipple Observatory Tillinghast 1.5-m telescope. ASAS-SN discoveries with new classifications include ASASSN-17ip, ASASSN-17jz, ASASSN-17mf, ASASSN-17oh, and ASASSN-17ot. We report all updated redshifts and classifications in Table 1.

We solved astrometry in follow-up images taken of all ASAS-SN supernovae using the astrometry.net package (Barron et al. 2008; Lang et al. 2010) and measured centroid positions for the SNe using IRAF. This generally results in errors of  $<1''.0$  in position, significantly more accurate than positions measured directly from ASAS-SN images, which have a  $7''.0$  pixel scale. Images used to measure astrometry were obtained using the Las Cumbres Observatory 1-m telescopes or by amateur collaborators who work with the ASAS-SN team. All coordinates announced in discovery ATels were measured from follow-up images in this way, and we report these coordinates in Table 1. The offsets between the SNe and the centers of their host galaxies are also reported in the Table, and these offsets were calculated using galaxy coordinates available in NED, or measured from archival images in cases where a host center was not previously catalogued.

We remeasured  $V$ -band, host-subtracted peak magnitudes from ASAS-SN data for all ASAS-SN supernova discoveries. In addition, as the three new units deployed last year use  $g$ -band filters, we also remeasured  $g$ -band peak magnitudes for each ASAS-SN supernova that was discovered after the new units were deployed. Both magnitudes are reported in Table 1. In some cases, due to the way ASAS-SN fields were divided between cameras and because the new units were still building reference images in late 2017, SNe were only detected in a single filter. We also report discovery magnitudes in the discovery filter measured from the re-subtracted light curves. In some cases, these magnitudes differ from the magnitudes reported in the original discovery ATels or on TNS, as re-reduction of the data has led to improvements in the photometry. As we did in the previous ASAS-SN catalogs, we define the ‘‘discovery magnitude’’ as the magnitude of the SN on the date it was discovered. For supernovae with enough detections in their light curves (for either or both filters), we also performed parabolic fits to the

<sup>2</sup> <https://wis-tns.weizmann.ac.il/>

<sup>3</sup> <https://ned.ipac.caltech.edu/>

<sup>4</sup> [gelato.tng.iac.es](http://gelato.tng.iac.es)

light curves and estimate peak magnitudes based on the fits. The “peak magnitude” for each filter reported in Table 1 is the brighter value between the peak of the parabolic fit and the brightest magnitude measured in the light curve.

As in Holoien et al. (2017a,b,c), all supernovae discovered by ASAS-SN in 2017 are included in this catalog, including those fainter than  $m_V = 17$  or  $m_g = 17$ . When performing comparison analyses that are presented in Section 3, we only include those ASAS-SN discoveries with  $m_{peak} \leq 17$  so that our sample is consistent with the non-ASAS-SN sample.

## 2.2 The Non-ASAS-SN Supernova Sample

Table 2 contains information for all spectroscopically confirmed SNe discovered by other professional and amateur SN searches between 2017 January 1 and 2017 December 31 with peak magnitudes of  $m_{peak} \leq 17$ .

As in our previous catalogs, the list of non-ASAS-SN discoveries was generated from the “latest supernovae” website<sup>5</sup> designed and maintained by D. W. Bishop (Gal-Yam et al. 2013). Discoveries reported via different channels (including TNS and ATels) are compiled on this website, and objects reported by different sources at different times are linked, making it an ideal source for information on supernovae discovered by different groups. As some supernova searches do not participate in the TNS system, we used TNS only for verifying data from the latest supernova website, and not as a primary source of information for non-ASAS-SN discoveries.

We obtained supernova names, IAU names, discovery dates, coordinates, host offsets, peak reported magnitudes, spectral types, and discovery sources for each supernovae in the non-ASAS-SN sample from the latest supernovae website, when possible. NED was used to gather host galaxy names and redshifts when available, with the SN redshifts on the latest supernova website being used in other cases. If a host offset was not listed on the website, the offset was taken from NED, with the offset being defined as the angular separation between the reported coordinates of the supernova and the galaxy coordinates in NED.

In some cases, a host galaxy was clearly visible in archival Pan-STARRS data (Chambers et al. 2016) despite no host galaxy being listed at the position of the host in NED. For such cases we used IRAF to measure a centroid position of the host to use to calculate the offset. All host galaxy names listed for both the ASAS-SN and non-ASAS-SN samples are the primary names of the host galaxies from NED, which in some cases differ from the names listed on the ASAS-SN supernova page or the latest supernova website.

The magnitudes from the latest supernovae website are reported in different filters from various telescopes, and in many cases the reported photometry does not necessarily cover the actual peak of the supernova light curve. For the purposes of having a more consistent sample of supernova peak magnitudes between the ASAS-SN sample, which uses peak magnitudes measured from ASAS-SN data, and the non-ASAS-SN sample, we also produced re-reduced, host-subtracted  $V$ - and  $g$ -band ASAS-SN light curves for every

non-ASAS-SN supernova in the 2017 sample. As we did with the ASAS-SN sample, we also performed parabolic fits to the light curves with enough detections, and used the brighter of the brightest measured magnitude and the peak of the fit as the peak magnitude for each filter, when a supernova was detected. These peak ASAS-SN  $V$ - and  $g$ -band magnitudes are also listed in Table 2 for each supernova that was detected. We find that only 9 supernovae from the 2017 non-ASAS-SN sample are not detected in this re-measurement despite 48 of these supernovae not being recovered during normal survey operations. This is likely due to better-quality light curves being produced in this re-reduction, and the fact that our re-reduction ensures no supernova light is contained in the reference image, and thus subtracted from the light curve.

We performed a similar re-reduction and peak magnitude measurement for each supernova in the 2014-2016 non-ASAS-SN samples, and use only ASAS-SN  $V$ -band magnitudes when looking at the peak magnitude distribution and sample completeness in Section 3. The ASAS-SN light curves for all supernovae in these samples will be released in a future manuscript (Ping et al., *in prep.*)

As we did with the ASAS-SN sample, we also re-checked the redshifts and classifications of the non-ASAS-SN supernovae using publicly available spectra on TNS and WISEREP. Based on our re-examination of these spectra, we update the classifications of ATLAS17cpj and ATLAS17evm and the redshift of ATLAS17cpj. In addition, the supernova SN 2017gjf has a measured redshift of  $z \sim 0.072$ , but has been publicly announced as being hosted in the galaxy UGC 11950, which has a redshift of  $z = 0.020541$ . This was likely done because UGC 11950 is the nearest catalogued galaxy to the SN, but based on the redshift discrepancy we believe it likely that SN 2017gjf was actually located in an uncatalogued background galaxy, and we update the host name in our sample accordingly. We assume the SN redshift of  $z \sim 0.072$  for SN 2017gjf in our analyses presented in Section 3. All updated types and redshifts are reported in Table 2.

For all supernovae discovered by other professional surveys, we list the name of the discovery group in Table 2. We use “Amateurs” as the discovery source for supernovae discovered by non-professional astronomers, to differentiate these supernovae from those discovered by ASAS-SN and other professional surveys. Unlike in previous years, amateurs no longer account for the second largest number of bright supernova discoveries after ASAS-SN, with the ATLAS survey (Tonry 2011; Tonry et al. 2018) now holding that distinction. Amateurs still account for the third largest number of bright supernova discoveries in 2017, however, showing they are still a significant source of bright discoveries.

Finally, as in our previous catalogs, we also note in Table 2 whether or not the supernovae in the non-ASAS-SN sample were independently recovered by the ASAS-SN team during normal survey operations. This allows us to quantify the impact ASAS-SN has on the discovery of bright supernovae in the absence of other supernova searches.

## 2.3 The Host Galaxy Samples

For both supernova samples, we collected Galactic extinction estimates in the directions of the host galaxies and host

<sup>5</sup> <http://www.rochesterastronomy.org/snimages/>

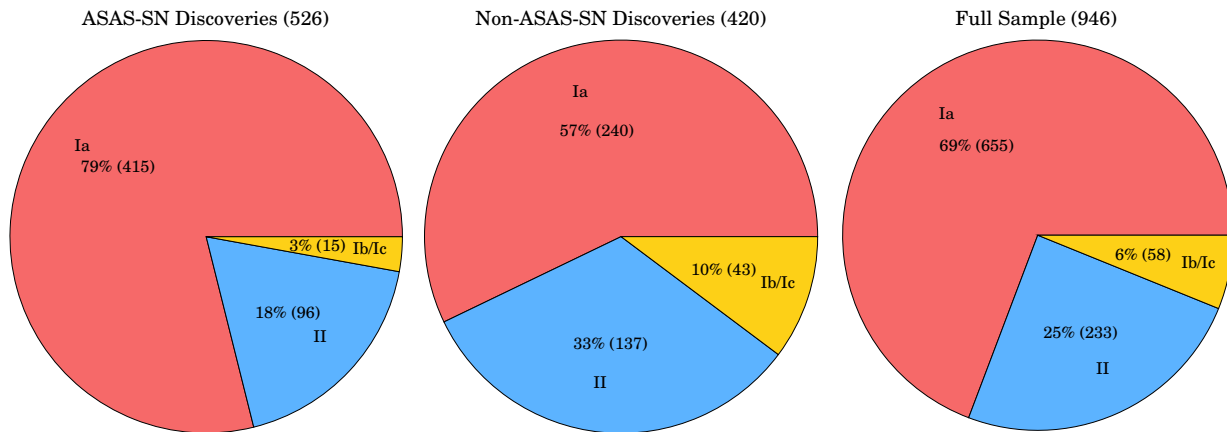


**Figure 1.** *Left Panel:* Breakdown of supernovae discovered by ASAS-SN by type between 2014 May 01 and 2017 December 31. The proportion of each type continues to very closely match that of an ideal magnitude-limited sample, as defined by Li et al. (2011). *Center Panel:* The same breakdown for the non-ASAS-SN sample over the the same time period. *Right Panel:* The breakdown of types for our entire combined supernova sample, now totaling 946 SNe. This analysis excludes the 3 superluminous supernovae in the sample, and includes Type IIb supernovae in the “Type II” sample.

magnitudes spanning from the near-ultraviolet (NUV) to the infrared (IR) wavelengths. These data are presented in Tables 3 and 4 for ASAS-SN hosts and non-ASAS-SN hosts, respectively. We obtained the values of Galactic  $A_V$  from Schlafly & Finkbeiner (2011) in the directions of the supernovae from NED. NUV host magnitudes from the Galaxy Evolution Explorer (GALEX; Morrissey et al. 2007) All Sky Imaging Survey (AIS), optical  $ugriz$  magnitudes from the Sloan Digital Sky Survey Data Release 14 (SDSS DR14; SDSS Collaboration et al. 2016), NIR  $JHK_S$  magnitudes from the Two-Micron All Sky Survey (2MASS; Skrutskie et al. 2006), and IR  $W1$  and  $W2$  from the Wide-field Infrared Survey Explorer (WISE; Wright et al. 2010) AllWISE source catalogs were obtained from publicly available online databases.

For host galaxies that were not detected in 2MASS, we adopted an upper limit in the  $J$  and  $H$  filters corresponding to our faintest detected host in our combined 2014 – 2017 sample ( $m_J > 17.0$ ,  $m_H > 16.4$ ). When hosts were not detected in 2MASS but were detected in WISE  $W1$  data, we estimated a  $K_S$  host magnitude by adding the mean  $K_S - W1$  offset from the combined sample to the WISE  $W1$  data. We calculated this mean offset by averaging the offsets for all hosts detected in both  $K_S$  and  $W1$  data from both the ASAS-SN and non-ASAS-SN samples from 2014 May 1 through 2017 December 31. This results in an average offset of  $-0.51$  magnitudes with a scatter of 0.04 magnitudes and a standard error of 0.002 magnitudes, matching the numbers we found when doing the same calculation for the 2014–2016 sample in Holoien et al. (2017c). For hosts not detected in either 2MASS or WISE data, we adopt an upper limit of  $m_{K_S} > 15.6$ , which corresponds to the faintest  $K_S$ -band host magnitude in our sample.

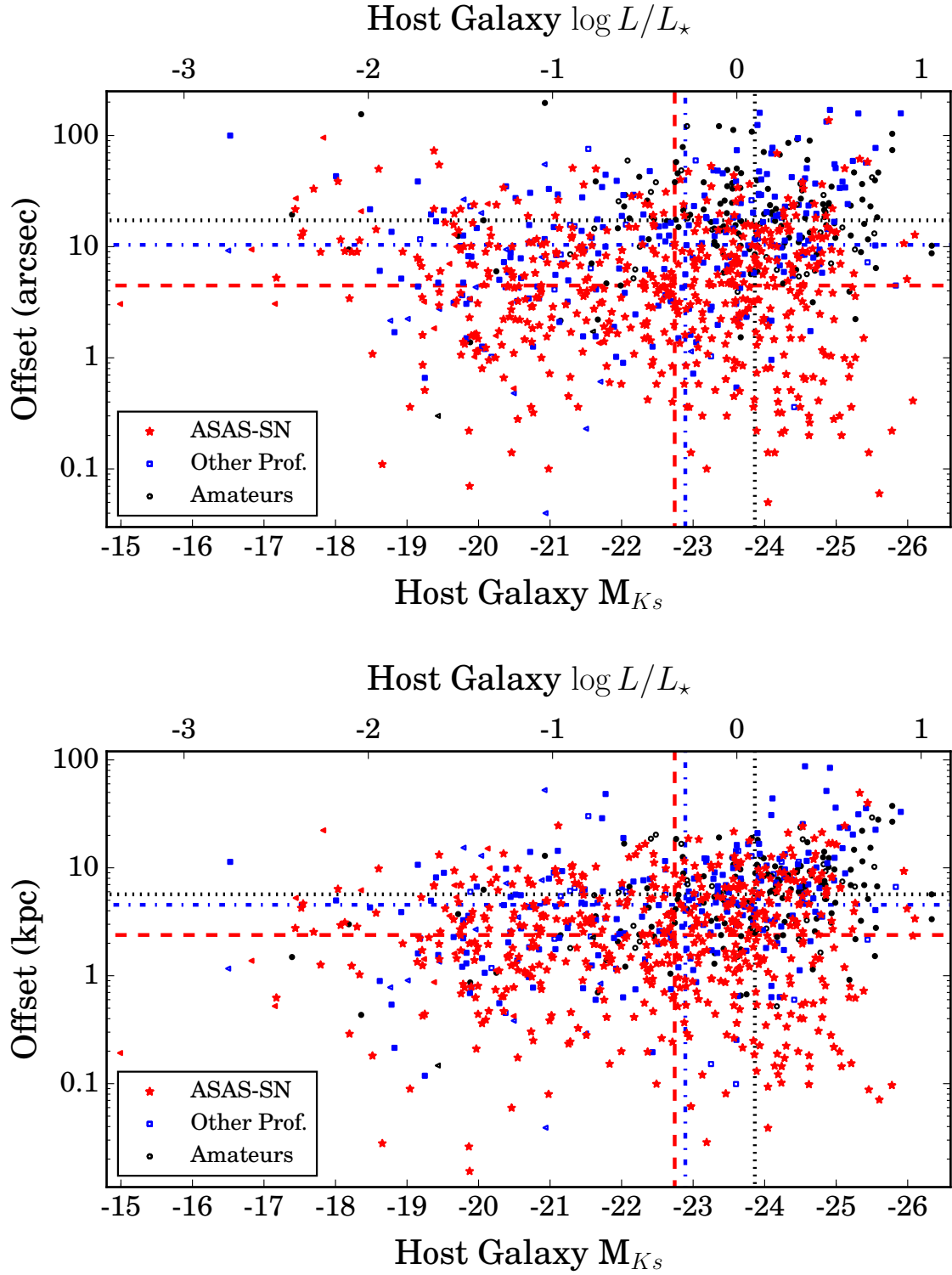
### 3 ANALYSIS OF THE SAMPLE

The total sample of bright supernovae discovered by all sources between 2014 May 01, when ASAS-SN began oper-

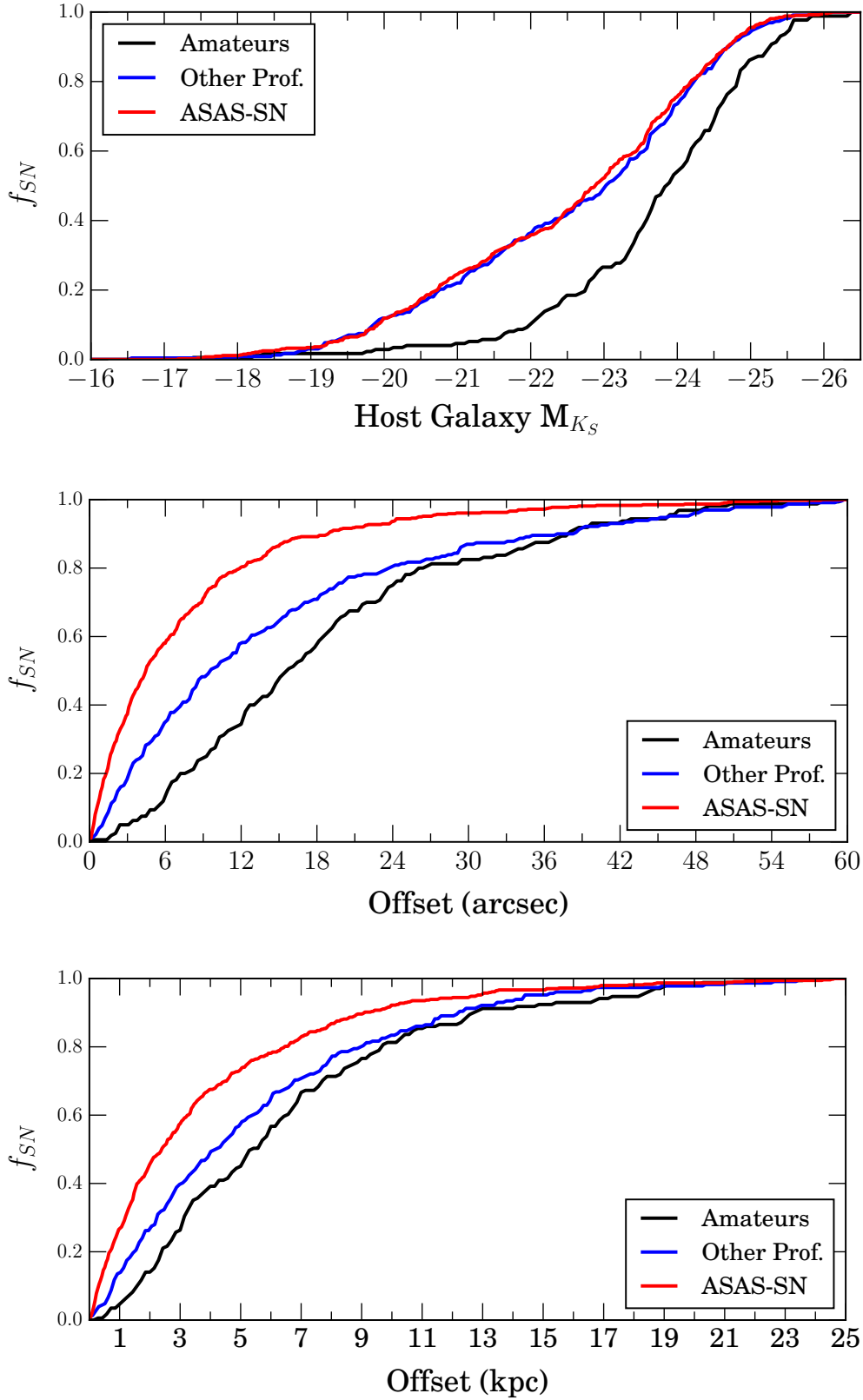
ations in the Southern hemisphere, and 2017 December 31 now includes 949 supernovae, after excluding ASAS-SN discoveries with  $m_{peak,V} > 17.0$  and  $m_{peak,g} > 17.0$  (Holoien et al. 2017a,b,c). 56% (528) of these supernovae were ASAS-SN discoveries, 19% (176) were discovered by amateur astronomers, and 26% (245) were discovered by other professional surveys. Breaking the sample down by type, 655 were Type Ia supernovae, 233 were Type II supernovae, 58 were type Ib/Ic supernovae, and 3 were superluminous supernovae. For the purpose of these analyses, we consider Type IIb supernovae as part of the Type II sample so that we can more directly compare with the results of Li et al. (2011), as we have done in our previous catalogs. The object ASASSN-15lh, either an extremely luminous Type I SLSN (Dong et al. 2016; Godoy-Rivera et al. 2017) or a tidal disruption event (Leloudas et al. 2016), is excluded from the following analysis.

Figure 1 shows the breakdown by type of the supernovae in the ASAS-SN, non-ASAS-SN, and total samples. As is expected for a magnitude-limited sample (e.g., Li et al. 2011), Type Ia supernovae represent the largest fraction in each of the three samples. As we have seen in our previous catalogs, the ASAS-SN sample continues to match the “ideal magnitude-limited sample” predicted from the LOSS sample in Li et al. (2011), where there are 79% Type Ia, 17% Type II, and 4% Type Ib/Ic, almost exactly. Due to the observing strategies of the various discovery sources in the non-ASAS-SN sample not necessarily being magnitude-limited in all cases (e.g., because the survey targets certain types of galaxies or takes a volume-limited approach), the other two samples have higher fractions of core-collapse supernovae than the ASAS-SN sample.

ASAS-SN accounts for 56% of the bright supernovae in our total sample, and thus remains the dominant source of bright supernova discoveries despite new surveys like ATLAS coming online in 2017. A large fraction of the ASAS-SN sample continues to be discovered shortly after explosion because of our high cadence. Of the 459 ASAS-SN discoveries with approximate discovery ages, 70% (322) were discov-



**Figure 2.** *Upper Panel:* The offset of all supernovae in our 2014 – 2017 combined sample from their host nuclei in arcseconds compared to the absolute  $K_S$ -band host magnitude. The  $\log(L/L_*)$  values that correspond to the magnitude range shown on the bottom scale are shown on the top axis, assuming  $M_{*,K_S} = -24.2$  (Kochanek et al. 2001). Red stars, black circles, and blue squares denote ASAS-SN discoveries, amateur discoveries, and other professional discoveries, respectively. Upper limits on the host galaxy magnitudes for hosts that are not detected in 2MASS or WISE are indicated with triangles in corresponding colors. Filler points indicate supernovae that were discovered or independently recovered by ASAS-SN. The median host magnitudes and offsets are indicated with dashed, dotted, and dash-dotted lines for ASAS-SN discoveries, amateur discoveries, and other professional discoveries, respectively, in colors that correspond to those of the matching data points. *Lower Panel:* As above, but with the offset measured in kiloparsecs.



**Figure 3.** Cumulative, normalized distributions of host galaxy absolute magnitudes (upper panel), offset from host nucleus in arcseconds (center panel), and offset from host nucleus in kpc (bottom panel) for the ASAS-SN supernova sample (red), the other professional sample (blue), and the amateur sample (black). As is seen in Figure 2, amateur discoveries are biased towards more luminous hosts than professional surveys, and ASAS-SN continues to find supernovae at smaller offsets than either comparison group, regardless of how the offset is measured.

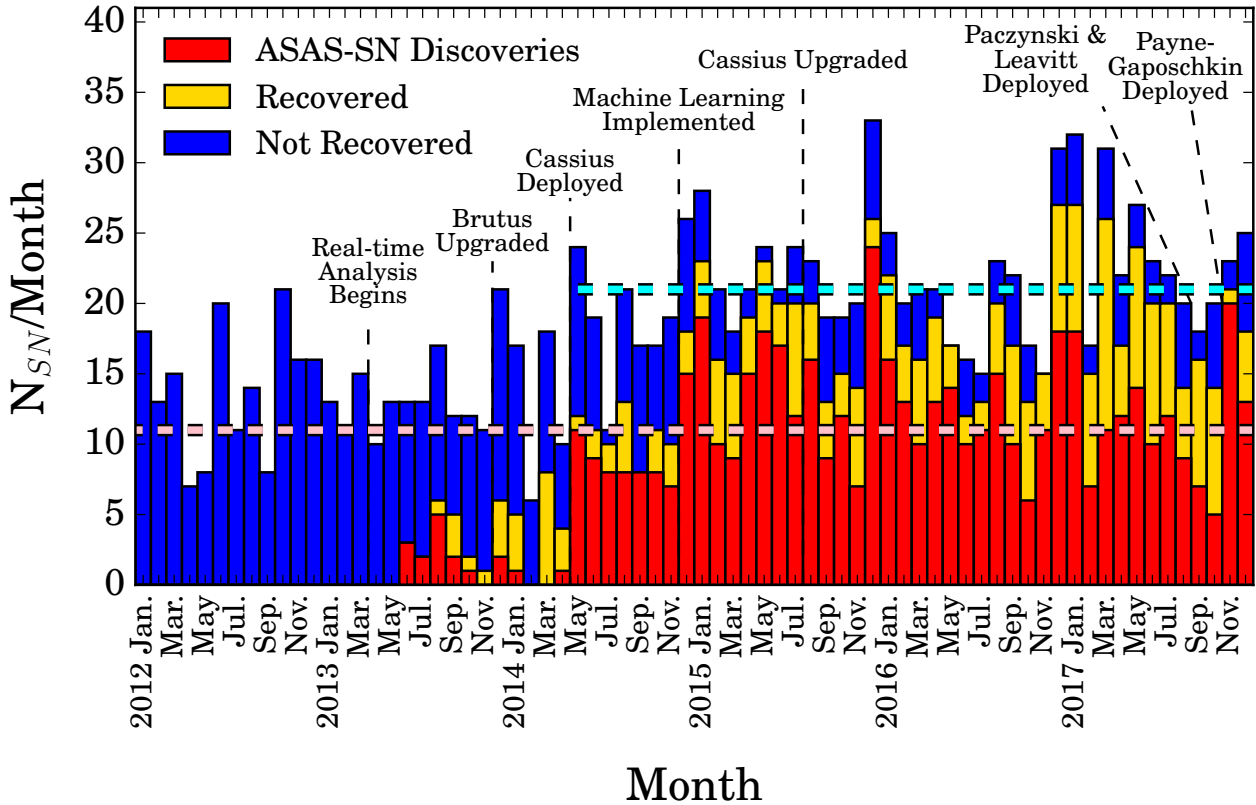


**Figure 4.** Histogram of bright supernovae discovered in each month from 2012 through 2017. ASAS-SN discoveries are shown in red, supernovae found by other sources and recovered in ASAS-SN data are shown in yellow, and supernovae not recovered by ASAS-SN (or discovered prior to ASAS-SN coming online) are shown in blue. Significant milestones in the ASAS-SN timeline are indicated. The dashed pink line indicates the median number of bright supernovae discovered in each month from 2010 through 2012, while the dashed cyan line indicates the median number of bright supernovae discovered in each month since 2014 May. Since ASAS-SN became operational in both hemispheres in 2014 May, the number of bright supernova discoveries has exceeded the previous median and supernovae discovered or recovered by ASAS-SN account for more than half of all bright supernova discoveries in every month.

ered prior to reaching their peak brightness. As we found in Holoien et al. (2017b) and Holoien et al. (2017c), the ASAS-SN sample is less affected by host galaxy selection effects than other bright supernovae searches: 24% (127) of the ASAS-SN discoveries were found in catalogued hosts without previously available redshift measurements in NED and an additional 4% (19) were found in uncatalogued hosts or were hostless. In contrast, 18% (74) of non-ASAS-SN discoveries were discovered in catalogued hosts without reported redshifts, and only 2% (9) were found in uncatalogued hosts or were hostless.

Figure 2 shows the host galaxy  $K_S$ -band absolute magnitudes compared to the offsets of the supernovae from their host centers for all supernovae in our sample. The Figure shows the ASAS-SN, amateur, and other professional samples as different colors, and also shows the median offsets and magnitudes for each source. We also give a luminosity scale corresponding to the magnitude scale to put the magnitude scale in perspective, assuming that an  $L_*$  galaxy has  $M_{*,K_S} = -24.2$  (Kochanek et al. 2001).

As we have seen in the previous ASAS-SN catalogs, amateur discoveries are significantly biased towards more luminous hosts and larger offsets from the host galaxy nucleus (Holoien et al. 2017a,b,c). This is unsurprising given that

amateur supernova searches tend to observe the brightest, nearest galaxies and use less sophisticated detection techniques than professional surveys. Discoveries made by other professional surveys continue to exhibit a smaller median angular separation than amateur discoveries (median value of  $10''.4$  compared to  $17''.3$ ), and now show a smaller median offset in physical separation as well (4.5 kpc vs. 5.7 kpc). This is in contrast to previous years, when the median physical offset was similar between the two groups (e.g., Holoien et al. 2017c). ASAS-SN remains less biased against discoveries close to the host nucleus than either group, with the ASAS-SN discoveries showing median offsets of  $4''.5$  and 2.4 kpc.

The median host galaxy magnitude for ASAS-SN discoveries is  $M_{K_S} \simeq -22.7$ , compared to  $M_{K_S} \simeq -22.9$ , and  $M_{K_S} \simeq -23.9$  for other professional surveys and amateurs, respectively. This is similar to the trend we have seen in our previous years' catalogs, where there is a clear distinction in host luminosity between professional surveys (including ASAS-SN) and amateurs (Holoien et al. 2017a,b,c).

The cumulative distributions of host galaxy magnitudes and offsets from host nuclei are shown in Figure 3. The Figure shows clearly that the amateur supernova sample stands out from the ASAS-SN and other professional samples in



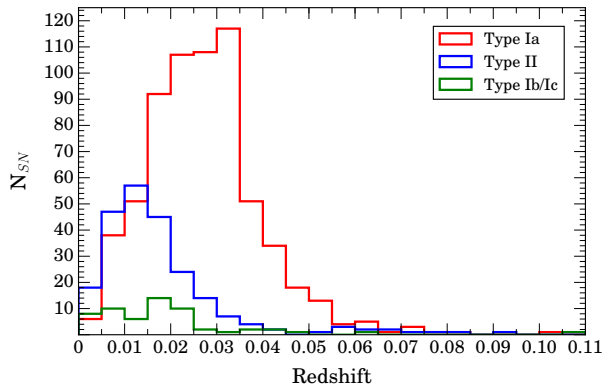


**Figure 5.** Histograms of redshifts of the supernovae in our complete sample with a bin width of  $z = 0.005$ . We show the distributions for Type Ia (red line), Type II (blue line), and Type Ib/Ic (green line) separately. Type Ia supernovae are largely found at higher redshifts than the core-collapse supernovae, as they are typically more luminous.

host galaxy luminosity. It also shows that supernovae discovered by ASAS-SN are more concentrated towards the centers of their hosts, and that those discovered by other professionals fall between the ASAS-SN sample and the amateur sample in offset. A larger fraction of the other professional sample was discovered by surveys that use difference imaging in 2017, largely due to the ATLAS survey. While ASAS-SN remains the dominant source of bright supernova discoveries, ATLAS has now surpassed amateur astronomers to become the second largest contributor of bright supernova discoveries. Despite the contribution of ATLAS, ASAS-SN continues to find supernovae with smaller median offsets than its competitors, and still has a smaller median offset than other professionals ( $3''.2$  vs.  $8''.6$ ) when looking only at 2017 discoveries. This implies that avoidance of central regions of galaxies remains relatively common in surveys other than ASAS-SN.

In Figure 4 we show the number of bright supernovae discovered in each month from 2012 through 2017 in order to show the impact ASAS-SN has on the discovery of bright supernovae. Various milestones in the history of ASAS-SN, such as the deployment of additional units and software improvements, are also shown in the figure to show the impact of these changes.

In Holoien et al. (2017c) we showed that ASAS-SN had little impact on the number of bright supernovae being discovered per month in its first year of operation: From 2012 January through 2013 May, the average number of bright supernovae found per month was 13 with a scatter of 4 supernovae per month, and the average was 15 with a scatter of 5 supernovae per month from 2013 June through 2014 May. After our expansion to the southern hemisphere and improvements to our pipeline, our detection efficiency and cadence improved dramatically, and this had a significant impact on the number of supernovae found per month. In the months since 2014 May, the average number of bright supernovae found per month has increased to 21 with a scatter of 5 supernovae per month, indicating ASAS-SN has increased the rate of bright supernovae found per month. The addition of the 2017 sample has only improved the trend from Holoien

et al. (2017c), as the average rate is now  $\sim 21 \pm 2$ , rather than  $\sim 20 \pm 2$  as was seen in the 2016 catalog. While the addition of new surveys like ATLAS has cut into the number of ASAS-SN discoveries somewhat, ASAS-SN still discovered or recovered well over half of all bright supernovae every month in 2017. ASAS-SN continues to find supernovae that would not be found if it did not exist, and this is allowing us to construct a more complete sample of bright supernovae.

The distribution of redshifts of the supernovae in our complete sample, shown in Figure 5, has not changed significantly from Holoien et al. (2017c). The Type Ia distribution peaks between  $z = 0.03$  and  $z = 0.035$ , the Type II distribution peaks between  $z = 0.01$  and  $z = 0.015$ , and the Type Ib/Ic distribution peaks between  $z = 0.015$  and  $z = 0.02$ . As we noted in our previous catalogs, this distribution is not unexpected given that we have a mostly magnitude-limited sample since Type Ia supernovae are more luminous on average than core-collapse supernovae.

Finally, in Figure 6 we show a cumulative histogram of supernova peak magnitudes for ASAS-SN discoveries, supernovae discovered or recovered by ASAS-SN, and all supernovae in our complete sample. Because the magnitudes from the Bright Supernova website are from different sources and in different filters, for the purposes of this figure we use only supernovae for which we were able to obtain an ASAS-SN  $V$ -band light curve. This allows us to look at our completeness with a consistent set of peak magnitudes that come from the same telescopes and same filters. This also allows this sample to be more easily applied to supernova rate studies.

The majority of very bright ( $m_{peak} \lesssim 14.5$ ; Holoien et al. 2017b) supernovae are discovered by amateurs or the Distance Less Than 40 Mpc (DLT40) survey<sup>6</sup>, both of which typically survey the brightest and nearest galaxies rather than taking an unbiased, all-sky approach. However, ASAS-SN recovers the vast majority of these supernovae, and in 2017 ASAS-SN discovered or recovered every supernova with  $m_{peak} < 15.3$ , a significant improvement from 2016, when we only discovered or recovered everything with  $m_{peak} < 14.3$  (Holoien et al. 2017c).

Figure 6 also gives an illustration of the estimated completeness of our sample. We used a broken power-law fit, shown as a green dashed line in the Figure, to model the distribution of the observable supernovae brighter than  $m_{peak} = 17.01$ . This fit assumes a Euclidean slope below the break magnitude and a variable slope above it. We used Markov Chain Monte Carlo methods to derive the parameters of the fit. Similar to what we found in the 2016 catalog, we find that the best-fit break magnitude is  $m = 16.24 \pm 0.11$  for the complete sample, meaning that the number counts are consistent with a Euclidean slope for magnitudes brighter than 16.24.

The integral completeness of our total sample relative to Euclidean predictions is  $0.95 \pm 0.03$  at  $m = 16.5$  and  $0.73 \pm 0.03$  at  $m = 17.0$ . The differential completeness relative to Euclidean predictions is  $0.71 \pm 0.07$  at  $m = 16.5$  and  $0.36 \pm 0.04$  at  $m = 17.0$ . These results are very similar to what we found in Holoien et al. (2017c) and imply that roughly 70% of the supernovae brighter than  $m_{peak} = 17$  and roughly 30% of the  $m_{peak} = 17$  supernovae are being

<sup>6</sup> <http://dark.physics.ucdavis.edu/dlt40/DLT40>

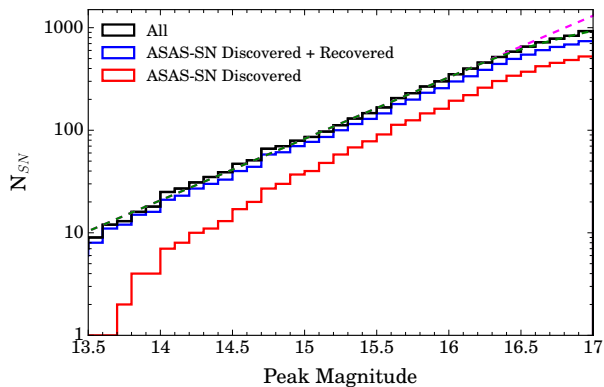


**Figure 6.** Cumulative histogram of peak supernovae  $V$ -band magnitudes with a 0.1 magnitude bin width. ASAS-SN discoveries are shown with a red line, supernovae discovered or recovered by ASAS-SN are shown with a blue line, and all supernovae in the sample are shown with a black line. The broken power-law fit shown with a green dashed line has been normalized to the complete sample, and has a Euclidean slope below the break magnitude and a variable slope above it. The magenta dashed line shows the Euclidean slope extrapolated to  $m = 17$ , and the sample is approximately 70% complete for  $m_{peak} < 17$ . Only supernovae with ASAS-SN  $V$ -band light curves are included in this Figure.

found. We note that the Euclidean approximation we use for this analysis does not take into account any deviations from Euclidean geometry,  $K$ -corrections, or effects of time dilation on supernova rates, so it likely underestimates the true completeness for faint supernovae slightly. We will include these higher order corrections when carrying out a full analysis of nearby supernova rates.

#### 4 CONCLUSIONS

This manuscript presents a comprehensive catalog of spectroscopically confirmed bright supernovae and their hosts, totaling 308 new supernovae discovered in 2017. Our total combined bright supernova sample now includes 949 supernovae, with 528 of these discovered by ASAS-SN and an additional 216 independently recovered by ASAS-SN after discovery. The ASAS-SN sample remains extremely similar to that of an ideal magnitude-limited sample from Li et al. (2011), while the combined sample has a similar distribution but with a larger proportion of core-collapse supernovae relative to Type Ia supernovae than expected.

ASAS-SN remains the only professional survey to provide a complete, rapid-cadence, all-sky survey of nearby transients, and with the expansion of our telescope network in 2017, it will have an even greater impact on the discovery and follow-up of bright supernovae going forward. The ATLAS survey is now the primary competition to ASAS-SN for new discoveries, though amateur astronomers still discover a significant fraction of the brightest supernovae and discover the third most supernovae in our 2017 sample overall. Despite the advent of recent professional surveys like ATLAS, ASAS-SN continues to find supernovae closer to galactic nuclei than its competitors (Figure 2), and finds supernovae that would not be found otherwise (Figure 4). ASAS-SN re-

covered the majority of bright supernovae that it did not discover in 2017, as was the case in 2015 and 2016, and it recovered or discovered all supernovae with  $m_{peak} \leq 15.3$  in 2017.

Similar to what we found in Holoien et al. (2017c), our total sample is roughly complete to a peak magnitude of  $m_{peak} = 16.2$ , and is roughly 70% complete for  $m_{peak} \leq 17.0$ . This analysis served as the precursor to our first supernova rates paper, where we found that the specific Type Ia supernova rate rises as host galaxy mass decreases (Brown et al. 2018). Manuscripts with further rate calculations with respect to other host properties (e.g., star formation rate and metallicity) and an overall nearby supernova rate paper are in preparation, and will have a significant impact on a number of fields of astronomy, including the nearby core-collapse rate (e.g., Horiuchi et al. 2011, 2013) and multi-messenger studies ranging from gravitational waves (e.g., Ando et al. 2013; Nakamura et al. 2016), to MeV gamma rays from Type Ia supernovae (e.g., Horiuchi & Beacom 2010; Diehl et al. 2014; Churazov et al. 2015) to GeV–TeV gamma rays and neutrinos from rare types of core-collapse supernovae (e.g., Ando & Beacom 2005; Murase et al. 2011; Abbasi et al. 2012). Joint measurements such as these will greatly increase the scientific reach of ASAS-SN.

This is the fourth of a yearly series of catalogs of bright supernovae and their hosts provided by the ASAS-SN team. It is our hope that these catalogs will provide useful data repositories for bright supernova and host galaxy properties that can be used for new and interesting population studies. As ASAS-SN continues to dominate the discovery of the best and brightest transients in the sky, this is just one way in which we can use our unbiased sample to impact supernova research.

#### ACKNOWLEDGMENTS

The authors thank Las Cumbres Observatory and its staff for their continued support of ASAS-SN.

ASAS-SN is supported by the Gordon and Betty Moore Foundation through grant GBMF5490 to the Ohio State University and NSF grant AST-1814440. Development of ASAS-SN has been supported by NSF grant AST-0908816, the Center for Cosmology and AstroParticle Physics at the Ohio State University, the Mt. Cuba Astronomical Foundation, the Chinese Academy of Sciences South America Center for Astronomy (CASSACA), and by George Skestos.

This material is based upon work supported by the National Science Foundation Graduate Research Fellowship Program Under Grant No. DGE-1343012. JSB, KZS, and CSK are supported by NSF grant AST-181440. KZS and CSK are also supported by NSF grant AST-1515876. Support for JLP is provided in part by FONDECYT through the grant 1151445 and by the Ministry of Economy, Development, and Tourism’s Millennium Science Initiative through grant IC120009, awarded to The Millennium Institute of Astrophysics, MAS. SD, SB, and PC acknowledge Project 11573003 supported by NSFC. JFB is supported by NSF grant PHY-1714479. MDS is supported by generous grants provided by the Danish Agency for Science and Technology and Innovation realized through a Sapere Aude Level 2 grant and the Villum foundation. TAT is supported in part

by Scialog Scholar grant 24215 from the Research Corporation. PRW acknowledges support from the US Department of Energy as part of the Laboratory Directed Research and Development program at LANL.

This research uses data obtained through the Telescope Access Program (TAP), which has been funded by “the Strategic Priority Research Program-The Emergence of Cosmological Structures” of the Chinese Academy of Sciences (Grant No.11 XDB09000000) and the Special Fund for Astronomy from the Ministry of Finance.

This research has made use of the XRT Data Analysis Software (XRTDAS) developed under the responsibility of the ASI Science Data Center (ASDC), Italy. At Penn State the NASA *Swift* program is support through contract NAS5-00136.

This research was made possible through the use of the AAVSO Photometric All-Sky Survey (APASS), funded by the Robert Martin Ayers Sciences Fund.

This research has made use of data provided by Astronomy.net (Barron et al. 2008; Lang et al. 2010).

This paper uses data products produced by the OIR Telescope Data Center, supported by the Smithsonian Astrophysical Observatory.

Observations made with the NASA Galaxy Evolution Explorer (GALEX) were used in the analyses presented in this manuscript. Some of the data presented in this paper were obtained from the Mikulski Archive for Space Telescopes (MAST). STScI is operated by the Association of Universities for Research in Astronomy, Inc., under NASA contract NAS5-26555. Support for MAST for non-HST data is provided by the NASA Office of Space Science via grant NNX13AC07G and by other grants and contracts.

Funding for SDSS-III has been provided by the Alfred P. Sloan Foundation, the Participating Institutions, the National Science Foundation, and the U.S. Department of Energy Office of Science. The SDSS-III web site is <http://www.sdss3.org/>.

This publication makes use of data products from the Two Micron All Sky Survey, which is a joint project of the University of Massachusetts and the Infrared Processing and Analysis Center/California Institute of Technology, funded by NASA and the National Science Foundation.

This publication makes use of data products from the Wide-field Infrared Survey Explorer, which is a joint project of the University of California, Los Angeles, and the Jet Propulsion Laboratory/California Institute of Technology, funded by NASA.

This research is based in part on observations obtained at the Southern Astrophysical Research (SOAR) telescope, which is a joint project of the Ministério da Ciência, Tecnologia, e Inovação (MCTI) da República Federativa do Brasil, the U.S. National Optical Astronomy Observatory (NOAO), the University of North Carolina at Chapel Hill (UNC), and Michigan State University (MSU).

The Liverpool Telescope is operated on the island of La Palma by Liverpool John Moores University in the Spanish Observatorio del Roque de los Muchachos of the Instituto de Astrofísica de Canarias with financial support from the UK Science and Technology Facilities Council.

This research has made use of the NASA/IPAC Extragalactic Database (NED), which is operated by the Jet

Propulsion Laboratory, California Institute of Technology, under contract with NASA.

## REFERENCES

- Abbasi R., et al., 2012, *A&A*, **539**, A60
- Ando S., Beacom J. F., 2005, *Physical Review Letters*, **95**, 061103
- Ando S., et al., 2013, *Reviews of Modern Physics*, **85**, 1401
- Balam D. D., Thanjavur K., Hsiao E. Y., 2017, *The Astronomer’s Telegram*, **10646**
- Baltay C., et al., 2013, *PASP*, **125**, 683
- Barbarino C., et al., 2017, *The Astronomer’s Telegram*, **10094**
- Barron J. T., Stumm C., Hogg D. W., Lang D., Roweis S., 2008, *AJ*, **135**, 414
- Bersier D., 2017a, *The Astronomer’s Telegram*, **10162**
- Bersier D., 2017b, *The Astronomer’s Telegram*, **10209**
- Berton M., et al., 2018, *The Astronomer’s Telegram*, **11171**
- Blondin S., Tonry J. L., 2007, *ApJ*, **666**, 1024
- Bock G., et al., 2017, *The Astronomer’s Telegram*, **10279**
- Bose S., Dong S., Klusmeyer J., Prieto J. L., Shields J., Stanek K. Z., 2017a, *The Astronomer’s Telegram*, **10047**
- Bose S., Chen P., Dong S., 2017b, *The Astronomer’s Telegram*, **11113**
- Bose S., et al., 2018a, preprint, ([arXiv:1810.12304](https://arxiv.org/abs/1810.12304))
- Bose S., et al., 2018b, *ApJ*, **862**, 107
- Bose S., Chen P., Dong S., Bersier D., Prieto J. L., 2018c, *The Astronomer’s Telegram*, **11163**
- Brimacombe J., et al., 2017a, *The Astronomer’s Telegram*, **9939**
- Brimacombe J., et al., 2017b, *The Astronomer’s Telegram*, **9951**
- Brimacombe J., et al., 2017c, *The Astronomer’s Telegram*, **9965**
- Brimacombe J., et al., 2017d, *The Astronomer’s Telegram*, **9998**
- Brimacombe J., et al., 2017e, *The Astronomer’s Telegram*, **9999**
- Brimacombe J., et al., 2017f, *The Astronomer’s Telegram*, **10000**
- Brimacombe J., et al., 2017g, *The Astronomer’s Telegram*, **10100**
- Brimacombe J., et al., 2017h, *The Astronomer’s Telegram*, **10135**
- Brimacombe J., et al., 2017i, *The Astronomer’s Telegram*, **10199**
- Brimacombe J., et al., 2017j, *The Astronomer’s Telegram*, **10232**
- Brimacombe J., et al., 2017k, *The Astronomer’s Telegram*, **10255**
- Brimacombe J., et al., 2017l, *The Astronomer’s Telegram*, **10300**
- Brimacombe J., et al., 2017m, *The Astronomer’s Telegram*, **10358**
- Brimacombe J., et al., 2017n, *The Astronomer’s Telegram*, **10370**
- Brimacombe J., et al., 2017o, *The Astronomer’s Telegram*, **10463**
- Brimacombe J., et al., 2017p, *The Astronomer’s Telegram*, **10555**
- Brimacombe J., et al., 2017q, *The Astronomer’s Telegram*, **10652**
- Brimacombe J., et al., 2017r, *The Astronomer’s Telegram*, **10662**
- Brimacombe J., et al., 2017s, *The Astronomer’s Telegram*, **10695**
- Brimacombe J., et al., 2017t, *The Astronomer’s Telegram*, **10760**
- Brimacombe J., et al., 2017u, *The Astronomer’s Telegram*, **10796**
- Brimacombe J., et al., 2017v, *The Astronomer’s Telegram*, **10883**
- Brimacombe J., et al., 2017w, *The Astronomer’s Telegram*, **10897**
- Brimacombe J., et al., 2017x, *The Astronomer’s Telegram*, **10930**
- Brimacombe J., et al., 2017y, *The Astronomer’s Telegram*, **10960**
- Brimacombe J., et al., 2017z, *The Astronomer’s Telegram*, **10992**
- Brimacombe J., et al., 2017aa, *The Astronomer’s Telegram*, **11018**
- Brimacombe J., et al., 2017ab, *The Astronomer’s Telegram*, **11035**
- Brimacombe J., et al., 2017ac, *The Astronomer’s Telegram*, **11074**
- Brimacombe J., et al., 2017ad, *The Astronomer’s Telegram*, **11103**
- Brimacombe J., et al., 2018, *The Astronomer’s Telegram*, **11145**
- Brown T. M., et al., 2013, *PASP*, **125**, 1031
- Brown J. S., Shappee B. J., Holoiën T. W.-S., Stanek K. Z., Kochanek C. S., Prieto J. L., 2016, *MNRAS*, **462**, 3993
- Brown J. S., Holoiën T. W.-S., Auchtell K., Stanek K. Z., Kochanek C. S., Shappee B. J., Prieto J. L., Grupe D., 2017a, *MNRAS*, **466**, 4904
- Brown J. S., et al., 2017b, *The Astronomer’s Telegram*, **9952**
- Brown J. S., et al., 2017c, *The Astronomer’s Telegram*, **10474**
- Brown J. S., et al., 2018, preprint, ([arXiv:1810.00011](https://arxiv.org/abs/1810.00011))

- Bufano F., et al., 2018, *The Astronomer's Telegram*, [11135](#)
- Cacella P., et al., 2017, *The Astronomer's Telegram*, [10280](#)
- Cannizzaro G., Kostrzewa-Rutkowska Z., Stritzinger M., Dong S., Benetti S., Fraser M., Rasmussen R. T., 2017, *The Astronomer's Telegram*, [10298](#)
- Chambers K. C., et al., 2016, preprint, ([arXiv:1612.05560](#))
- Churazov E., et al., 2015, *ApJ*, [812](#), 62
- Cikota A., et al., 2017, *The Astronomer's Telegram*, [9945](#)
- Diehl R., et al., 2014, *Science*, [345](#), 1162
- Dong S., et al., 2016, *Science*, [351](#), 257
- Dong S., et al., 2017, *The Astronomer's Telegram*, [10320](#)
- Drake A. J., et al., 2009, *ApJ*, [696](#), 870
- Drout M. R., Holoien T. W.-S., Shappee B. J., 2017, *The Astronomer's Telegram*, [10014](#)
- Elias-Rosa N., et al., 2017, *The Astronomer's Telegram*, [10344](#)
- Fabricant D., Cheimets P., Caldwell N., Geary J., 1998, *PASP*, [110](#), 79
- Farfan R. G., et al., 2017, *The Astronomer's Telegram*, [10614](#)
- Foley R. J., Jones D. O., Siebert M. R., 2017, *The Astronomer's Telegram*, [10976](#)
- Fraser M., et al., 2017, *The Astronomer's Telegram*, [10212](#)
- Frieman J. A., et al., 2008, *AJ*, [135](#), 338
- Gal-Yam A., Mazzali P. A., Manulis I., Bishop D., 2013, *PASP*, [125](#), 749
- Godoy-Rivera D., et al., 2017, *MNRAS*, [466](#), 1428
- Gorbovskoy E. S., et al., 2013, *Astronomy Reports*, [57](#), 233
- Hamanowicz A., Gromadzki M., Wyrzykowski L., Buckley D., 2017, *The Astronomer's Telegram*, [10424](#)
- Harutyunyan A. H., et al., 2008, *A&A*, [488](#), 383
- Herczeg G. J., et al., 2016, preprint, ([arXiv:1607.06368](#))
- Hodgkin S. T., Wyrzykowski L., Blagorodnova N., Kopusov S., 2013, *Philosophical Transactions of the Royal Society of London Series A*, [371](#), 20120239
- Holoien T. W.-S., et al., 2014a, *MNRAS*, [445](#), 3263
- Holoien T. W.-S., et al., 2014b, *ApJ*, [785](#), L35
- Holoien T. W.-S., et al., 2016a, *Acta Astron.*, [66](#), 219
- Holoien T. W.-S., et al., 2016b, *MNRAS*, [455](#), 2918
- Holoien T. W.-S., et al., 2016c, *MNRAS*, [463](#), 3813
- Holoien T. W.-S., et al., 2017a, *MNRAS*, [464](#), 2672
- Holoien T. W.-S., et al., 2017b, *MNRAS*, [467](#), 1098
- Holoien T. W.-S., et al., 2017c, *MNRAS*, [471](#), 4966
- Holoien T. W.-S., Brown J. S., Auchettl K., Kochanek C. S., Prieto J. L., Shappee B. J., Van Saders J., 2018, *MNRAS*, [480](#), 5689
- Horiuchi S., Beacom J. F., 2010, *ApJ*, [723](#), 329
- Horiuchi S., Beacom J. F., Kochanek C. S., Prieto J. L., Stanek K. Z., Thompson T. A., 2011, *ApJ*, [738](#), 154
- Horiuchi S., Beacom J. F., Bothwell M. S., Thompson T. A., 2013, *ApJ*, [769](#), 113
- Hossein-zadeh G., Arcavi I., Howell D. A., McCully C., Valenti S., 2017a, *The Astronomer's Telegram*, [10112](#)
- Hossein-zadeh G., Arcavi I., Howell D. A., McCully C., Valenti S., 2017b, *The Astronomer's Telegram*, [10269](#)
- Hossein-zadeh G., Arcavi I., Howell D. A., McCully C., Valenti S., 2017c, *The Astronomer's Telegram*, [10365](#)
- Hossein-zadeh G., Arcavi I., McCully C., Howell D. A., Valenti S., 2017d, *The Astronomer's Telegram*, [10410](#)
- Hossein-zadeh G., McCully C., Valenti S., Arcavi I., Howell D. A., 2017e, *The Astronomer's Telegram*, [10579](#)
- Kaiser N., et al., 2002, in Tyson J. A., Wolff S., eds, *Proceedings of the SPIE Vol. 4836, Survey and Other Telescope Technologies and Discoveries*. pp 154–164, [doi:10.1117/12.457365](#)
- Kankare E., et al., 2017a, *The Astronomer's Telegram*, [10391](#)
- Kankare E., et al., 2017b, *The Astronomer's Telegram*, [10846](#)
- Kato T., et al., 2014a, *PASJ*, [66](#), 30
- Kato T., et al., 2014b, *PASJ*, [66](#), 90
- Kato T., et al., 2015, *PASJ*, [67](#), 105
- Kato T., et al., 2016, *PASJ*, [68](#), 65
- Kilpatrick C. D., Pan Y.-C., Foley R. J., Jha S. W., Rest A., Scolnic D., 2017, *The Astronomer's Telegram*, [10032](#)
- Kiyota S., et al., 2017, *The Astronomer's Telegram*, [10122](#)
- Kochanek C. S., et al., 2001, *ApJ*, [560](#), 566
- Kostrzewa-Rutkowska Z., et al., 2017, *The Astronomer's Telegram*, [10834](#)
- Krannich G., et al., 2017, *The Astronomer's Telegram*, [10022](#)
- Lang D., Hogg D. W., Mierle K., Blanton M., Roweis S., 2010, *AJ*, [139](#), 1782
- Law N. M., et al., 2009, *PASP*, [121](#), 1395
- Leloudas G., et al., 2016, *Nature Astronomy*, [1](#), 0002
- Li W. D., et al., 2000, in Holt S. S., Zhang W. W., eds, *American Institute of Physics Conference Series Vol. 522, American Institute of Physics Conference Series*. pp 103–106 ([arXiv:astro-ph/9912336](#)), [doi:10.1063/1.1291702](#)
- Li W., et al., 2011, *MNRAS*, [412](#), 1441
- Lin H., Xiang D., Rui L., Wang X., Xiao F., Zhang T., Zhang J., 2017, *The Astronomer's Telegram*, [11090](#)
- Lopez K. M., et al., 2017, *The Astronomer's Telegram*, [11022](#)
- Masi G., et al., 2017a, *The Astronomer's Telegram*, [9989](#)
- Masi G., et al., 2017b, *The Astronomer's Telegram*, [10544](#)
- Morrell N., Shappee B., Drout M., Dong S., 2017, *The Astronomer's Telegram*, [10240](#)
- Morrissey P., et al., 2007, *ApJS*, [173](#), 682
- Murase K., Thompson T. A., Lacki B. C., Beacom J. F., 2011, *Physical Review D*, [84](#), 043003
- Nakamura K., Horiuchi S., Tanaka M., Hayama K., Takiwaki T., Kotake K., 2016, *MNRAS*, [461](#), 3296
- Nicholls B., et al., 2017, *The Astronomer's Telegram*, [10339](#)
- Nyholm A., et al., 2017, *The Astronomer's Telegram*, [9980](#)
- Pan Y.-C., Takaro T., Chowdhury R., Foley R. J., Jha S. W., Rest A., Scolnic D., 2017, *The Astronomer's Telegram*, [10225](#)
- Pignata G., et al., 2009, in Giobbi G., Tornambe A., Raimondo G., Limongi M., Antonelli L. A., Menci N., Brocato E., eds, *American Institute of Physics Conference Series Vol. 1111, American Institute of Physics Conference Series*. pp 551–554 ([arXiv:0812.4923](#)), [doi:10.1063/1.3141608](#)
- Post R. S., et al., 2017a, *The Astronomer's Telegram*, [9944](#)
- Post R. S., et al., 2017b, *The Astronomer's Telegram*, [9948](#)
- Post R. S., et al., 2017c, *The Astronomer's Telegram*, [9957](#)
- Post R. S., et al., 2017d, *The Astronomer's Telegram*, [10084](#)
- Prieto J. L., et al., 2016, preprint, ([arXiv:1609.00013](#))
- Quimby R. M., 2006, PhD thesis, The University of Texas at Austin
- Rodriguez O., Prieto J. L., 2017, *The Astronomer's Telegram*, [10580](#)
- Romero-Cañizales C., Prieto J. L., Chen X., Kochanek C. S., Dong S., Holoien T. W.-S., Stanek K. Z., Liu F., 2016, preprint, ([arXiv:1609.00010](#))
- Rui L., Wang X., Xiang D., Wu H., Jia J., Zhai M., Zhang T., Zhang J., 2017, *The Astronomer's Telegram*, [9997](#)
- SDSS Collaboration et al., 2016, preprint, ([arXiv:1608.02013](#))
- Schlafly E. F., Finkbeiner D. P., 2011, *ApJ*, [737](#), 103
- Schmidt S. J., et al., 2014, *ApJ*, [781](#), L24
- Schmidt S. J., et al., 2016, *ApJ*, [828](#), L22
- Shappee B. J., et al., 2014, *ApJ*, [788](#), 48
- Shappee B. J., et al., 2016, *ApJ*, [826](#), 144
- Skrutskie M. F., et al., 2006, *AJ*, [131](#), 1163
- Smith M., et al., 2017, *The Astronomer's Telegram*, [11062](#)
- Stone G., et al., 2017a, *The Astronomer's Telegram*, [10146](#)
- Stone G., et al., 2017b, *The Astronomer's Telegram*, [10156](#)
- Stone G., et al., 2017c, *The Astronomer's Telegram*, [10431](#)
- Strader J., Chomiuk L., Tremou L., Dong S., 2017, *The Astronomer's Telegram*, [10591](#)
- Taddia F., et al., 2017, *The Astronomer's Telegram*, [9968](#)
- Tonry J. L., 2011, *PASP*, [123](#), 58
- Tonry J. L., et al., 2018, *PASP*, [130](#), 064505
- Tucker M. A., et al., 2018, preprint, ([arXiv:1808.07875](#))

- Uddin S., Mould J., Zhang J.-J., Wang L., Wang X., 2017a, The Astronomer's Telegram, [10504](#)
- Uddin S., Mould J., Zhang J.-J., Tucker B., Wang L., Wang X., 2017b, The Astronomer's Telegram, [10517](#)
- Uddin S., Mould J., Zhang J.-J., Wang X., Wang L., 2017c, The Astronomer's Telegram, [10605](#)
- Vallely P. J., et al., 2018, *MNRAS*, [475](#), 2344
- Wang L., et al., 2017, The Astronomer's Telegram, [10727](#)
- Wiethoff W., et al., 2017, The Astronomer's Telegram, [10521](#)
- Wright E. L., et al., 2010, *AJ*, [140](#), 1868
- Wyrzykowski L., et al., 2014, *Acta Astron.*, [64](#), 197
- Yaron O., Gal-Yam A., 2012, *PASP*, [124](#), 668

**Table 1.** ASAS-SN Supernovae

SN Name	IAU Name	Discovery Date	RA <sup>a</sup>	Dec. <sup>a</sup>	Redshift	$m_b^{peak}$	$V_c^{peak}$	$g_{peak}^{peak}$	Offset (arcsec) <sup>d</sup>	Type at Disc. <sup>e</sup>	Age	Host Name <sup>f</sup>	Discovery ATel	Classification ATel
ASASSN-17ac	2017ad	2017-01-04.36	14:34:26.01	-38:28:09.70	0.03332	16.6	16.3	—	6.09	Ia	-6	2MASX J14342552	Brimacombe et al. (2017a)	Cikota et al. (2017)
ASASSN-17ad	2017ah	2017-01-04.55	11:10:01.95	+63:38:34.16	0.03286	17.3	15.9	—	3.82	Ia	-11	CGCG 314-011	Post et al. (2017a)	TNS
ASASSN-17ae	2017aj	2017-01-04.66	16:17:02.62	+10:41:36.17	0.02627	17.5	17.6	—	11.50	Ia	-3	2MASX J16170338	Brimacombe et al. (2017b)	TNS
ASASSN-17af	2017bc	2017-01-05.51	12:19:50.90	-06:51:20.45	0.02687	17.0	16.4	—	4.47	Ia	-4	MCG -01-32-001	Brimacombe et al. (2017b)	Cikota et al. (2017)
ASASSN-17ai	2017bl	2017-01-09.63	12:07:18.83	+16:50:26.02	0.02307	17.3	16.7	—	4.74	Ib	-7	KUG 1204+171	Brown et al. (2017b)	Taddia et al. (2017)
ASASSN-17aj	2017hm	2017-01-09.62	11:33:10.50	-10:13:18.37	0.02128	16.9	15.8	—	25.50	Ia	-13	MCG -02-30-003	Brown et al. (2017b)	TNS
ASASSN-17ak	2017hq	2017-01-10.66	13:49:23.81	+08:30:27.62	0.03798	17.6	16.5	—	2.21	Ia	18	CGCG 073-079	Post et al. (2017c)	TNS
ASASSN-17ap	2017je	2017-01-03.11	00:37:37.59	-34:29:49.24	0.04500	17.4	16.8	—	8.94	Ia	-10	GALEXASC J003737	Brimacombe et al. (2017c)	Drout et al. (2017)
ASASSN-17aq	2017kf	2017-01-19.54	11:38:33.66	+25:23:50.17	0.02536	16.7	16.4	—	3.08	Ia	-9	2MASX J11383367	Masi et al. (2017a)	Nyholm et al. (2017)
ASASSN-17bb	2017ng	2017-01-23.65	15:20:40.75	+04:39:34.42	0.03700	16.9	16.7	—	1.86	Ia	-3	2MASX J15204087	Brimacombe et al. (2017d)	Drout et al. (2017)
ASASSN-17bc	2017nh	2017-01-23.36	07:10:13.52	+27:12:09.97	0.06100	17.6	16.8	—	6.18	Ia	1	2MASX J07101346	Brimacombe et al. (2017e)	Rui et al. (2017)
ASASSN-17bd	2017nk	2017-01-23.61	15:59:18.43	+13:36:50.89	0.03455	17.3	17.1	—	3.00	Ia	3	2MASX J15591838	Brimacombe et al. (2017f)	Drout et al. (2017)
ASASSN-17be	2017pa	2017-01-17.07	02:03:10.53	-61:41:10.61	0.04000	17.5	17.0	—	0.51	Ia	-1	2MASX J02031063	Brimacombe et al. (2017f)	Brimacombe et al. (2017f)
ASASSN-17bf	2017pb	2017-01-26.61	16:03:51.70	+39:59:24.17	0.03186	16.6	15.8	—	14.52	Ia	-3	CGCG 223-033	Drout et al. (2017)	Kilpatrick et al. (2017)
ASASSN-17bn	2017vu	2017-01-21.43	08:59:23.92	-09:52:29.32	0.04451	17.6	17.0	—	0.61	Ia	-2	2MASX J08592386	Kilpatrick et al. (2017)	Kilpatrick et al. (2017)
ASASSN-17bo	2017wb	2017-01-28.59	11:01:19.53	+70:39:54.76	0.03000	16.9	16.3	—	1.91	Ia	-9	2MASX J11011991	Krannich et al. (2017)	Krannich et al. (2017)
ASASSN-17bp	2017wi	2017-01-29.05	02:02:08.63	-17:59:56.36	0.05100	17.2	17.0	—	3.45	Ia	7	GALEXASC J020208	Krannich et al. (2017)	Bose et al. (2017a)
ASASSN-17bq	2017xx	2017-01-27.51	07:25:38.21	+59:00:09.63	0.04000	17.6	16.4	—	1.51	Ia	19	GALEXASC J072538	Krannich et al. (2017)	Krannich et al. (2017)
ASASSN-17br	2017yy	2017-01-29.63	15:52:00.31	+66:18:55.27	0.02600	17.1	18.1	—	3.71	IIP	10	GALEXASC J155200	Krannich et al. (2017)	Kilpatrick et al. (2017)
ASASSN-17bs	2017yh	2017-01-30.66	17:52:06.13	+21:33:57.82	0.02040	16.5	15.9	—	13.02	Ia	-8	IC 1269	Kilpatrick et al. (2017)	Bose et al. (2017a)

This table is available in its entirety in a machine-readable form in the online journal. A portion is shown here for guidance regarding its form and content.

<sup>a</sup> Right ascension and declination are given in the J2000 epoch.

<sup>b</sup> Discovery magnitudes are given in the  $V$ - or  $g$ -band from ASAS-SN, depending on the camera used for discovery.

<sup>c</sup> Peak  $V$ - and  $g$ -band magnitudes are measured from ASAS-SN data. “—” indicates a supernova was not detected in that filter.

<sup>d</sup> Offset indicates the offset of the supernova in arcseconds from the coordinates of the host nucleus, taken from NED.

<sup>e</sup> Discovery ages are given in days relative to peak. All ages are approximate and are only listed if a clear age was given in the classification telegram.

<sup>f</sup> “2MASX” and “GALEXASC” host names have been abbreviated due to space constraints.

**Table 2.** Non-ASAS-SN Supernovae

SN Name	IAU Name	Discovery Date	RA <sup>a</sup>	Dec. <sup>a</sup>	Redshift	$m_b^{peak}$	$V_c^{peak}$	$g_{peak}^{peak}$	Offset (arcsec) <sup>d</sup>	Type	Host Name	Discovered By <sup>e</sup>	Recovered? <sup>f</sup>
ATLAS17abh	2017ae	2017-01-04.29	02:05:50.62	+18:22:30.23	0.02200	16.4	16.2	—	4.74	Ia	GALEXASC J020550	ATLAS	Yes
2017hr	2017-01-06.69	23:06:27.39	+28:08:19.70	0.02930	16.6	17.0	—	1.38	Ia	Ia	SDSS J120627.46	Amateurs	Yes
PS17hj	2017-01-09.21	12:34:36.47	-04:32:04.32	0.007368	14.6	—	—	1.26	Ia	Ia	IC 5334	Pan-STARRS	No
2017hn	2017-01-09.41	13:07:39.46	+06:20:14.60	0.023853	16.1	15.8	—	4.66	Ia	Ia	UGC 08204	Amateurs	Yes
ATLAS17ajn	2017-01-14.63	11:44:26.54	-28:27:27.22	0.028717	17.0	16.7	—	18.48	Ia	Ia	ESO 440-G001	ATLAS	Yes
MASTER OT J081506.13+381123.3	2017-01-16.02	08:15:16.13	+38:11:23.30	0.054000	16.9	16.6	—	11.35	Ia	Ia	2MASX J08150520	MASTER	No
ATLAS17air	2017-01-16.22	00:57:31.90	+30:11:06.83	0.016331	14.6	15.3	—	5.88	Ia	Ia	2MASX J00573150	ATLAS	Yes
2017mf	2017-01-21.09	14:16:31.0	+39:35:12.02	0.025678	16.0	15.9	—	12.6	Ia	Ia	NGC 5541	Amateurs	Yes
PTSS-17dfe	2017-01-21.71	10:26:42.37	+36:40:50.62	0.024639	15.6	15.7	—	5.22	Ia	Ia	SDSS J102641.99	PTSS	Yes
ATLAS17akw	2017-01-23.21	23:53:31.13	+03:44:08.18	0.038800	16.8	—	—	34.38	Ia-91T	Ia	SSTSL2 J235328.89	ATLAS	No
ATLAS17alb	2017-01-23.31	02:49:10.36	+14:36:02.48	0.027900	16.7	—	—	2.88	Ia	Ia	2MASX J02491020	ATLAS	No
ATLAS17amz	2017-01-26.31	04:46:24.59	-11:59:18.25	0.014000	16.5	15.8	—	0	IIP	IIP	Uncatalogued	ATLAS	No
ATLAS17auc	2017-01-26.64	13:32:42.09	-21:48:04.35	0.02947	15.9	15.9	—	1.38	Ia	Ia	2MASX J13324217	ATLAS	Yes
ATLAS17aux	2017-01-30.65	13:43:23.25	-19:56:37.13	0.030000	16.9	16.1	—	3.84	Ia	Ia	GALEXASC J134322	ATLAS	Yes
Gaia17aiq	2017-02-00.43	09:49:56.70	+67:10:59.56	0.01305	16.0	16.2	—	38.6	IIP	IIP	KUG 0945+674	Gaia	Yes
DLT17h	2017-02-08.36	10:37:17.45	-41:37:05.27	0.009255	15.8	15.3	—	40.32	II	II	NGC 3318	DLT40	Yes
MASTER OT J083256.92+035128.1	2017-02-11.93	08:32:56.92	-03:51:28.10	0.030584	16.5	16.5	—	5.82	Ia	Ia	2MASX J08325728	MASTER	Yes
PS17bbn	2017-02-14.58	13:05:3.01	+53:39:33.21	0.029037	17.0	16.7	—	19.44	Ia-91bg	Ia	CGCG 270-047	Pan-STARRS	Yes
iPTF17aub	2017-02-15.3	06:40:24.70	+64:33:02.75	0.016000	17.0	16.9	—	10.02	II	II	CGCG 308-036	PTF	No
ATLAS17bam	2017-02-16.32	05:20:47.08	+03:15:24.55	0.027426	16.4	16.4	—	23.46	Ia	Ia	CGCG 421-034	ATLAS	Yes

This table is available in its entirety in a machine-readable form in the online journal. A portion is shown here for guidance regarding its form and content.

<sup>a</sup> Right ascension and declination are given in the J2000 epoch.

<sup>b</sup> Magnitudes are taken from D. W. Bishop’s Bright Supernova website, as described in the text, and may be from different filters.

<sup>c</sup> All  $V$ - and  $g$ -band peak magnitudes are measured from ASAS-SN data for cases where the supernova was detected.

<sup>d</sup> Offset indicates the offset of the supernovae in arcseconds from the coordinates of the host nucleus, taken from NED.

<sup>e</sup> “Amateurs” indicates discovery by any number of non-professional astronomers, as described in the text.

<sup>f</sup> Indicates whether the supernova was independently recovered in ASAS-SN data or not.

**Table 3.** ASAS-SN Supernova Host Galaxies

Galaxy Name	Redshift	SN Name	SN Type	SN Offset (arcsec)	$AV^a$	$m_{NUV}^b$	$m_u^c$	$m_g^c$	$m_r^c$	$m_i^c$	$m_z^c$	$m_J^d$	$m_H^d$	$m_{K_S}^{d,e}$	$m_{W1}$	$m_{W2}$
2MASX J14342552-3828081	0.03332	ASASSN-17ac	Ia	6.09	0.280	—	—	—	—	—	—	13.56	0.07	12.74	0.07	12.41
CGCG 314-011	0.03286	ASASSN-17ad	Ia	3.82	0.032	19.70	0.12	16.05	0.01	13.51	0.00	13.12	0.00	12.86	0.00	12.83
2MASX J16170338+1041359	0.05027	ASASSN-17ae	Ia	11.50	0.166	19.02	0.07	17.81	0.04	16.41	0.00	15.76	0.00	15.17	0.02	11.89
MCG -01-32-001	0.02687	ASASSN-17af	Ia	4.47	0.102	16.92	0.02	—	—	—	—	—	—	—	—	14.46
KUG 1204-171	0.02307	ASASSN-17ai	Ib	4.74	0.129	17.50	0.04	—	—	—	—	—	—	—	—	11.88
MCG -02-30-003	0.02128	ASASSN-17aj	Ia	25.50	0.114	17.80	0.03	—	—	—	—	—	—	—	—	13.85
CGCG 073-079	0.03798	ASASSN-17ak	Ia	2.21	0.077	17.17	0.04	16.22	0.01	14.53	0.00	13.71	0.00	12.98	0.00	12.97
GALEXASC J003737.20-342957.7	0.04500	ASASSN-17ap	Ia	8.94	0.037	19.43	0.05	—	—	—	—	—	—	—	—	11.27
2MASX J11383367+2523532	0.02536	ASASSN-17at	Ia	3.08	0.075	—	—	—	—	—	—	—	—	—	—	11.18
2MASX J15204067+0439331	0.03000	ASASSN-17bb	Ia	1.86	0.121	19.07	0.08	18.49	0.06	17.17	0.01	16.27	0.01	16.06	0.01	15.44
2MASX J07101346+2712041	0.06100	ASASSN-17bc	Ia	6.18	0.169	0.129	0.02	16.46	0.01	15.65	0.00	15.24	0.00	14.81	0.01	13.87
2MASX J15391898+1336487	0.03455	ASASSN-17bd	Ia	3.00	0.129	17.42	0.02	16.46	0.01	15.65	0.00	15.24	0.00	14.81	0.01	13.87
2MASX J02031063-6141105	0.04000	ASASSN-17be	Ia	0.51	0.096	21.32	0.28	—	—	—	—	—	—	—	—	12.98
CGCG 223-033	0.03186	ASASSN-17bh	Ia	14.52	0.038	18.99	0.06	—	—	—	—	—	—	—	—	12.70
2MASX J08592386-0952291	0.04451	ASASSN-17bn	Ia	0.61	0.101	21.08	0.21	—	—	—	—	—	—	—	—	12.85
2MASX J11011991+7039548	0.03000	ASASSN-17bo	Ia	1.91	0.068	18.14	0.05	—	—	—	—	—	—	—	—	14.81
GALEXASC J020208.73-175958.3	0.05100	ASASSN-17bp	Ia	3.45	0.075	18.68	0.04	17.86	0.02	16.92	0.01	16.63	0.01	16.30	0.02	14.81
GALEXASC J072538.14+590010.5	0.04000	ASASSN-17bq	Ia	1.51	0.136	21.59	0.36	—	—	—	—	—	—	—	—	14.24
GALEXASC J155200.16+661851.6	0.02600	ASASSN-17br	IIP	3.71	0.075	—	—	—	—	—	—	—	—	—	—	14.24
IC 1269	0.02040	ASASSN-17bs	Ia	13.02	0.243	16.11	0.01	—	—	—	—	—	—	—	—	11.83

This table is available in its entirety in a machine-readable form in the online journal. A portion is shown here for guidance regarding its form and content. Uncertainty is given for all magnitudes, and in some cases is equal to zero.

<sup>a</sup> Galactic extinction taken from Schlafly & Finkbeiner (2011).

<sup>b</sup> No magnitude is listed for those galaxies not detected in GALEX survey data.

<sup>c</sup> No magnitude is listed for those galaxies not detected in SDSS data or those located outside of the SDSS footprint.

<sup>d</sup> For those galaxies not detected in 2MASS data, we assume an upper limit of the faintest galaxy detected in each band from our sample.

<sup>e</sup>  $K_S$ -band magnitudes marked with a "\*" indicate those estimated from the WISE W1-band data, as described in the text.

**Table 4.** Non-ASAS-SN Supernova Host Galaxies

Galaxy Name	Redshift	SN Name	SN Type	SN Offset (arcsec)	$AV^a$	$m_{NUV}^b$	$m_u^c$	$m_g^c$	$m_r^c$	$m_i^c$	$m_z^c$	$m_J^d$	$m_H^d$	$m_{K_S}^{d,e}$	$m_{W1}$	$m_{W2}$
GALEXASC J020550.53	0.02200	ATLAS17abh	Ia	4.74	0.203	21.26	0.27	20.25	0.22	18.36	0.02	17.71	0.02	17.13	0.04	15.79
SDSS J120627.46+280820.6	0.029300	2017hr	Ia	1.38	0.061	—	—	—	—	—	—	—	—	—	—	17.0
IC 5334	0.007368	PS17hj	Ia	1.26	0.114	16.96	0.04	15.22	0.01	13.47	0.00	12.70	0.00	11.96	0.00	17.0
UGC 08204	0.023853	2017hn	Ia	4.66	0.091	17.35	0.04	16.03	0.01	14.54	0.00	13.79	0.00	13.38	0.00	11.02
ESO 440-G001	0.028717	ATLAS17aj	Ia	18.48	0.206	17.40	0.05	—	—	—	—	—	—	—	—	11.90
2MASX J08150520+3811205	0.054000	MASTER OT J081506	Ia	11.35	0.101	18.94	0.06	16.95	0.03	15.46	0.01	14.77	0.00	14.28	0.00	13.29
2MASX J00573150+3011098	0.016331	ATLAS17ar	Ia	5.88	0.201	19.21	0.08	18.20	0.04	16.72	0.00	16.03	0.00	15.71	0.00	14.74
NGC 5541	0.025678	2017mf	Ia	12.6	0.030	15.84	0.02	—	—	—	—	—	—	—	—	11.17
SDSS J102641.99+364053.2	0.024639	PTSS-17dfc	Ia	5.22	0.027	19.01	0.06	18.23	0.03	17.09	0.01	16.67	0.01	16.44	0.03	17.0
SSTSL2 J235328.89+034400	0.038800	ATLAS17akw	Ia-91T	34.38	0.136	—	—	—	—	—	—	—	—	—	—	11.70
2MASX J02491020+1436036	0.027900	ATLAS17alb	Ia	2.88	0.299	19.51	0.11	—	—	—	—	—	—	—	—	13.31
Uncatalogued	0.014000	ATLAS17amz	IIP	0	0.384	—	—	—	—	—	—	—	—	—	—	17.0
2MASX J13324217-2148034	0.02947	ATLAS17auc	Ia	1.38	0.232	19.34	0.10	—	—	—	—	—	—	—	—	13.66
GALEXASC J134322.97	0.030000	ATLAS17axb	Ia	3.84	0.300	20.96	0.33	—	—	—	—	—	—	—	—	17.0
KUG 0945+674	0.01305	Gai17aiq	IIB	40.32	0.212	—	—	—	—	—	—	—	—	—	—	17.0
NGC 3318	0.009255	DLT17h	II	40.32	0.212	—	—	—	—	—	—	—	—	—	—	17.0
2MASX J08325728-0351295	0.030584	MASTER OT J083256	Ia	5.82	0.100	20.41	0.14	17.32	0.02	15.47	0.00	14.64	0.00	14.25	0.00	10.07
CGCG 270-047	0.029037	PS17bn	Ia-91bg	19.44	0.052	18.50	0.06	16.41	0.01	14.60	0.00	13.83	0.00	13.11	0.00	12.70
CGCG 308-036	0.016000	iPTF17aub	II	10.02	0.229	17.59	0.03	16.44	0.02	15.11	0.00	14.49	0.00	14.18	0.00	13.33
CGCG 421-034	0.027426	ATLAS17bam	Ia	23.46	0.319	—	—	—	—	—	—	—	—	—	—	16.61

This table is available in its entirety in a machine-readable form in the online journal. A portion is shown here for guidance regarding its form and content. Uncertainty is given for all magnitudes, and in some cases is zero. "MASTER" supernova names and "GALEXASC" galaxy names have been abbreviated.

<sup>a</sup> Galactic extinction taken from Schlafly & Finkbeiner (2011).

<sup>b</sup> No magnitude is listed for those galaxies not detected in GALEX survey data.

<sup>c</sup> No magnitude is listed for those galaxies not detected in SDSS data or those located outside of the SDSS footprint.

<sup>d</sup> For those galaxies not detected in 2MASS data, we assume an upper limit of the faintest galaxy detected in each band from our sample.

<sup>e</sup>  $K_S$ -band magnitudes marked with a "\*" indicate those estimated from the WISE W1-band data, as described in the text.